small
NANO MICRO

Facile Synthesis of Bimetallic Ag/Ni Core/Sheath Nanowires and Their Magnetic and Electrical Properties

Maureen McKiernan, Jie Zeng, Sunzida Ferdous, Steven Verhaverbeke, Kurtis S. Leschkies, Roman Gouk, Christopher Lazik, Miao Jin, Alejandro L. Briseno, and Younan Xia,**

This paper describes a facile method for coating Ag nanowires with uniform, ferromagnetic sheaths made of polycrystalline Ni. A typical sample of these core/sheath nanowires had a saturation magnetization around 33 emu g^{-1}. We also demonstrated the use of this magnetic property to align the nanowires by simply placing a suspension of the nanowires on a substrate in a magnetic field and allowing the solvent to evaporate. The electrical conductivity of these core/sheath nanowires (2×10^3 S cm^{-1}) was two orders of magnitude lower than that of bulk Ag (6.3×10^5 S cm^{-1}) and Ni (1.4×10^5 S cm^{-1}). This is likely caused by the transfer of electrons from the Ag core to the Ni sheath due to the difference in work function between the two metals. The electrons are expected to experience an increased resistance due to spin-dependent scattering caused by the randomized magnetic domains in the polycrystalline, ferromagnetic Ni sheath. Studies on the structural changes to the Ni coating over time under different storage conditions show that storage of the nanowires on a substrate under ambient conditions leads to very little Ni oxidation after 6 months. These Ag/Ni core/sheath nanowires show promise in areas such as electronics, spintronics, and displays.

1. Introduction

One-dimensional (1D) nanostructures have received a great deal of attention over the past decade because of their unique anisotropic structure and fascinating physical properties.[1–8] These nanostructures show great promise in a wide range of applications such as electronics, photonics, sensing, imaging, drug delivery, and fabrication of solar cells.[1,9–13] Metallic 1D nanostructures, especially those made of Ag, are attractive for use in the manufacturing of electronic and display devices because of their superior electrical and thermal conductivity

Dr. J. Zeng, Prof. Y. Xia
Department of Biomedical Engineering
Washington University
St. Louis, MO 63130, USA
E-mail: zengj@seas.wustl.edu; xia@biomed.wustl.edu
M. McKiernan
Department of Chemistry, Washington University
St. Louis, MO 63130, USA
S. Ferdous, Prof. A. L. Briseno
Department of Polymer Science and Engineering
University of Massachusetts
Amherst, MA 01003, USA
S. Verhaverbeke, K. S. Leschkies, R. Gouk, C. Lazik, M. Jin
Applied Materials, Inc.
Santa Clara, CA 95054, USA

DOI: 10.1002/smll.201000801

in addition to their ability to act as optical waveguides.[14–17] Many such devices, however, require that the materials be manipulated and arranged over large areas. Methods have been developed to arrange nanowires into linear and other types of assemblies, but these methods generally require complex equipment and materials.[18,19] Simple magnetic manipulation has been demonstrated previously to arrange nanoparticles but has yet to be extended to nanostructures with very high aspect ratios such as Ag nanowires.[20] Therefore, there is still a need to design and synthesize 1D nanostructures that can be easily manipulated without the need for excessive equipment or labor.

Recently, there has been an increasing movement towards the integration of multiple materials into a single, hybrid nanostructure. These multicomponent nanostructures are attractive because of their increased functionality. By combining multiple materials into one structure we are combining their inherent physical properties as well as introducing an additional handle for tailoring the properties of a specific material. For example, Yu and co-workers have created Au-Fe_3O_4 hybrid nanostructures that incorporate both the optical properties of Au nanoparticles and the magnetic properties of Fe_3O_4 species.[21] Bimetallic nanostructures, in particular, have been shown to exhibit increased catalytic activity and greater plasmonic tunability than their monometallic counterparts.[22] Many different types of multicomponent nanostructures composed of semiconductors, metals or combinations of the two materials have been successfully synthesized with a wide variety of shapes and sizes.[23–26] In spite of this impressive success, it is worth pointing out that most of these syntheses cannot be readily extended to the production of 1D, bimetallic, core/sheath nanostructures. Difficulties arise because of three main reasons: i) the possibility for galvanic replacement between the two different metals; ii) the tendency for alloying between the metallic components; and iii) the surface of the nanowires tends to lack the rough features or active sites necessary for heterogeneous nucleation and growth compared to nanoparticles, which leads to the preference of homogeneous nucleation during synthesis. Therefore, a facile robust procedure is still desired for the preparation of 1D, bimetallic, core/sheath nanostructures. In this study, we aim to integrate ferromagnetic Ni with electrically conductive Ag in order to create multifunctional nanowires that can be assembled on a large scale and potentially applied to the construction of nanometer-scale devices and electronics.

Bimetallic Ag/Ni core/sheath nanowires have been synthesized previously using an anodic-aluminum oxide template method combined with electrochemical deposition of Ni.[27] Although this technique is useful because it can easily reduce Ni ions to elemental Ni, the procedure involves multiple steps and the diameter of the nanowires is limited by the pore size of the template. Our group has previously developed simple polyol methods for the synthesis of Ag nanowires with a range of diameters.[28,29] Our aim with this study is to coat these Ag nanowires using a simple, solution-based Ni deposition method. During the synthesis we characterized changes in surface morphology of the Ag/Ni nanowires using electron microscopy. We also confirmed the core/sheath structure of these Ag/Ni nanowires using cross-sectional transmission electron microscopy (TEM) imaging. We found that these nanowires are magnetically responsive by simply placing them in a magnetic field. We also found that their electrical conductivity was lower than that of bulk Ag and bulk Ni due to the metal/metal interface created and increased electron scattering in the core/sheath structure. Finally, we observed that the method by which the nanowires were stored affected their degree of surface oxidation over time and that storage on a substrate under ambient conditions leads to very little oxidation.

2. Results and Discussion

2.1. Synthesis of Ag/Ni Core/Sheath Nanowires

The Ag/Ni core/sheath nanowires were synthesized by a two-step procedure (**Figure 1**A). In the first step, Ag nanowires were synthesized using a previously published protocol with some minor modifications.[29] Similar to other polyol-based syntheses, ethylene glycol (EG) was used as both the solvent and source of reducing agent. A small amount of copper (II) chloride ($CuCl_2$) was added to the EG to increase the yield of nanowires. In addition, poly(vinyl pyrrolidone) (PVP) was added to serve as a capping agent, while silver nitrate ($AgNO_3$) was used as a source to elemental Ag. The reaction was visually monitored by its color changes and stopped once the

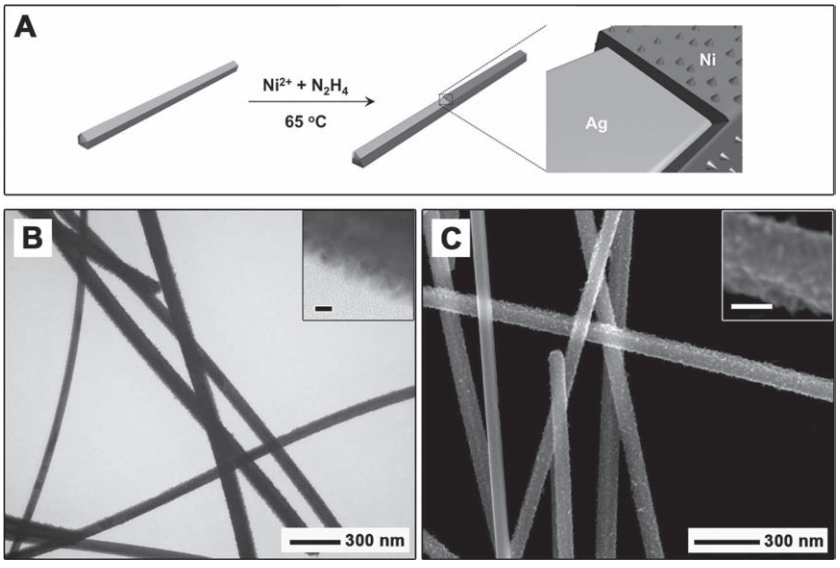

Figure 1. A) Scheme depicting the two-step synthesis of Ag/Ni core/sheath nanowires. B) TEM image of the final products. The inset is a TEM image at a higher magnification taken from the edge of a Ag/Ni nanowire (scale bar: 10 nm). C) SEM image of the final products. The inset shows an SEM image at a higher magnification taken from the edge of a nanowire, illustrating the rough surface (scale bar: 50 nm).

solution appeared light tan, wispy and opalescent. Figure S1 in the Supporting Information shows electron microscopy images of a typical sample of Ag nanowires. This $CuCl_2$-mediated synthesis generally yields about 90–95% Ag nanowires with an average diameter around 70 nm. From the inset of Figure S1A in the Supporting Information, the smooth surface of the Ag nanowires is clearly seen.

The second step of the synthesis involved the nucleation and growth of Ni on the surface of the Ag nanowires. We found that in order to produce a uniform coating of Ni on the Ag nanowire, a molar ratio of Ag precursor to Ni precursor around 16:11 was necessary. A range of molar ratios was attempted and we found that those samples with a lesser amount of Ni precursor did not produce a sufficient response to the magnetic field, while those samples with a higher amount of Ni precursor did not have uniform sheaths. The reduction of the Ni precursor in our synthesis was achieved by hydrazine monohydrate ($N_2H_4 \cdot H_2O$) according to the following reaction:

$$N_2H_4 \cdot H_2O \rightarrow N_2H_5^+ + OH^-$$
$$N_2H_5^+ + 2Ni^{2+} \rightarrow N_2 + 5H^+ + 2Ni \quad (1)$$

The products of the reaction were dark gray/black in color and tended to form large aggregates that adhered to the magnetic stir bar. After the final products were washed once with EG/acetone, they were easily re-dispersed in water and retained the wispy opalescence typical of metallic nanowires. It was observed that after a few minutes the nanowires began to aggregate and precipitate due to magnetic interactions between the Ag/Ni nanowires. Despite this aggregation, the nanowires could be easily re-dispersed in solution with slight agitation indicating that they do not form a permanent aggregate.

2.2. Structural Characterization

Figure 1B and C shows electron microscopy images of the as-prepared Ag/Ni nanowires. From these images we can conclude that these nanowires retained the original 1D morphology of the Ag nanowires in the core. The inset images in Figure 1 illustrate the change in surface morphology for the Ag nanowires after Ni coating. Compared to the Ag nanowires in Figure S1, the core/sheath nanowires have a rough, jagged surface due to the polycrystalline structure of the Ni coating. The nucleation and growth mechanism of Ni in this synthesis is much like that of a thin film grown on a substrate. In that case, there are three possible growth mechanisms: the Frank–van der Merwe (layer-by-layer), Volmer–Weber (island), and Stranski–Krastanov (island-on-layer) mechanisms.[30] The growth mechanism for a particular system is determined by the overall excess energy, $\Delta\gamma$. This overall energy is the sum of the surface energies of the materials and their interfacial and strain energies. In our system, it is defined by the following equation,

$$\Delta\gamma = \gamma_{Ni} + \gamma_i + \gamma_{strain} - \gamma_{Ag} \quad (2)$$

where, γ_{Ni} is the surface energy of Ni, γ_i is the energy of the interface formed by the two layers, γ_{strain} is the strain energy induced by the difference in lattice constants between the two layers, and γ_{Ag} is the surface energy of Ag. **Figure 2**A and B shows TEM images of Ag/Ni nanowires prepared with lower (Ag:Ni = 16:10) and higher (Ag:Ni = 16:12) amounts of added Ni precursor, respectively, than the standard sample (Ag:Ni = 16:11) shown in Figure 1. By comparing these images and those in Figure 1, we can conclude that the Ni sheath was formed by a Stranski–Krastanov (island-on-layer) growth mechanism. Initially, the Ni formed a homogeneous layer on the surface of the Ag nanowire (Figure 2A). The inset in Figure 2A shows a slightly roughened surface morphology compared to the inset in Figure S1A of the plain Ag nanowires. As the thickness of the Ni coating increased, the strain felt by the growing Ni layer due to the large lattice mismatch between the two metals induced a switch from layered growth to island growth. Figure 2B clearly shows that the sheath began to branch out and form dendrites rather than continue to form an even layer as more Ni was deposited.

To confirm the core/sheath morphology, we acquired a cross-sectional TEM image from a single Ag/Ni nanowire. In **Figure 3**A, we can clearly distinguish the highly crystalline Ag core with its pentagonally twinned structure from the polycrystalline Ni sheath. For this particular wire, the Ag core was about 70 nm in diameter with an even 5-nm-thick Ni sheath. We analyzed the composition of both the core and the sheath using energy-dispersive X-ray (EDX) analysis. The large difference in relative heights for the Ag and Ni peaks in the EDX spectra (Figure 3B and C) confirms that core and sheath were made of Ag and Ni, respectively. This result indicates that there was essentially no galvanic replacement or alloying taking place during or after the synthesis of the bimetallic nanowires.

2.3. Magnetic Properties

The magnetic properties of the Ag/Ni nanowires were explored using a variety of approaches. **Figure 4**A shows a magnetization curve for a sample of Ag/Ni nanowires. The curve follows the typical S-shape of a ferromagnetic material and the inset in Figure 4A shows an expanded region of

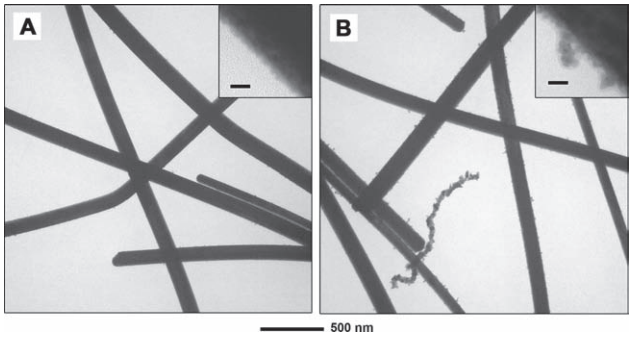

Figure 2. A) TEM image of Ag/Ni nanowires prepared with A) a lower amount (Ag/Ni = 16:10) and B) a higher amount (Ag/Ni = 16:12) of Ni precursor than the standard sample shown in Figure 1. The insets show TEM images at a higher magnification, illustrating the difference in surface morphology for the nanowires (scale bars: 20 nm).

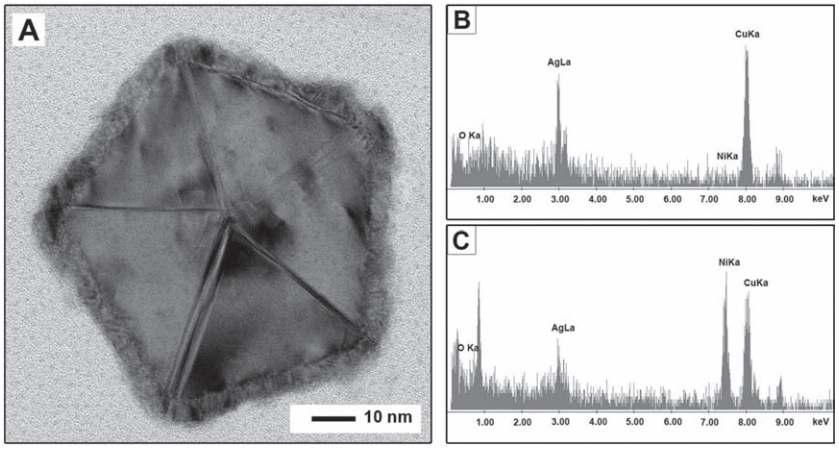

Figure 3. A) Cross-sectional TEM image of one of the Ag/Ni core/sheath nanowires shown in Figure 1. B,C) EDX spectra taken from the core and sheath of the nanowire, respectively. The small Ag peak in (C) is due to the spot size of the beam being around the same dimensions as the Ni sheath. The strong Cu peak is from the Cu TEM grid.

the curve that demonstrates the nonzero coercivity of these nanowires. This indicates that they are ferromagnetic rather than superparamagnetic. The critical diameter for superparamagnetic behavior in Ni nanoparticles has previously been determined to be 15 nm.[31] Although the thickness of the Ni coating on our Ag/Ni nanowires was only 5 nm, the lateral dimensions of the nanowires were much larger than the critical diameter of 15 nm. This large anisotropy creates multiple magnetic domains, which induces ferromagnetic behavior in the Ni sheaths. The saturation magnetization (M_s) of our sample was 33 emu g^{-1} where only the mass of Ni was considered. This value is lower than that of bulk Ni (58.57 emu g^{-1}), but larger than what was previously reported for pure Ni nanofibers (24.76 emu g^{-1}).[32,33] The reduction in M_s compared to bulk Ni could be due to the reduced thickness of the Ni sheath and/or surface oxidation. It has been shown previously that the saturation magnetization of Ni nanoparticles decreases with decreasing particle diameter.[34] It is likely that the Ni sheath of our Ag/Ni nanowires follows a similar trend. In addition, surface oxidation may lead to the creation of an antiferromagnetic NiO layer, which also limits the magnetic properties of our nanowires.[35] The coercivity of our Ag/Ni nanowires was 116 Oe, which is larger than that of bulk Ni (0.7 Oe). Compared to other 1D Ni nanostructures our value is slightly lower than that reported by Lin and co-workers for their Ag/Ni nanowires (180 Oe) and much lower than what has been reported for Ni nanotubes (200 Oe).[27,36,37] These values, however, are not directly comparable since the previously reported values were for arrays of nanowires or nanotubes, while the nanowires in our sample had no long-range order.

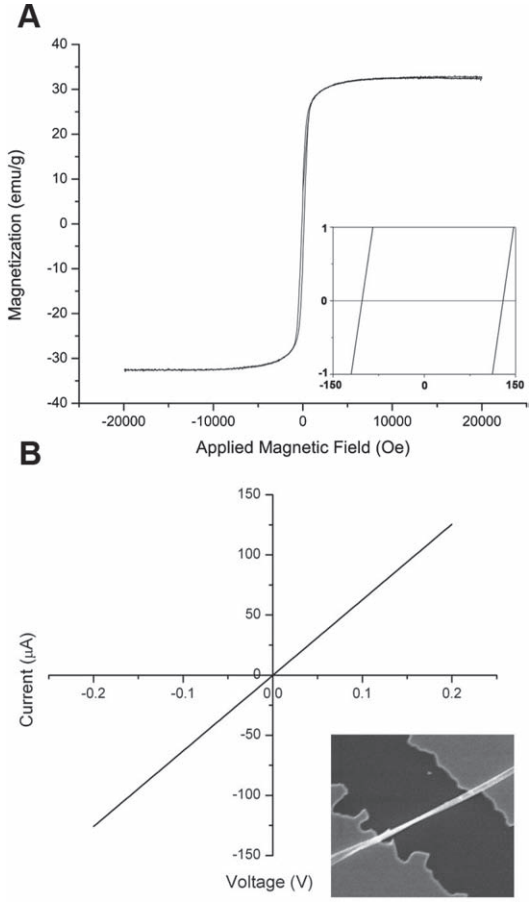

Figure 4. A) Magnetization curve for the Ag/Ni nanowires shown in Figure 1. The inset is an expanded view of the same curve depicting the nonzero coercivity of the nanowires. B) *I–V* curve of the Ag/Ni nanowires shown in Figure 1. The inset is an SEM image of the two nanowires spanning the electrode gap.

To demonstrate the magnetic properties of the Ag/Ni nanowires on a macroscopic scale, we observed their response to a small neodymium magnet. **Figure 5**A shows a digital photograph of the Ag/Ni nanowires dispersed in ethanol. The image suggests that despite the ferromagnetic behavior of these nanowires they could be easily dispersed in solution for further application. The image in Figure 5B is of the nanowires after resting overnight. It shows that the nanowires tend to aggregate due to their magnetic interactions and settle to the bottom of the vial. In Figure 5C, we see that the nanowires immediately respond to the magnetic field produced by the neodymium magnet, leaving behind a clear supernatant. This observation indicates that all nanowires in the solution had a sufficiently thick coating of Ni to respond to the external magnetic field.

Finally, we demonstrated the alignment of our Ag/Ni nanowires on a silicon substrate using a magnetic field as seen in Figure 5D. A small amount of the Ag/Ni nanowires in butyl alcohol was dropped onto a silicon wafer placed between opposite poles of a C-shaped magnet. From the scanning electron microscopy (SEM) image in Figure 5D, we find that the majority of the nanowires were aligned parallel to the magnetic field. A small number of nanowires, however, aligned perpendicular to the field direction. Some of the nanowires also seem to be aligned diagonal to the field direction. This unusual alignment is likely a result of the highly

small NANO MICRO

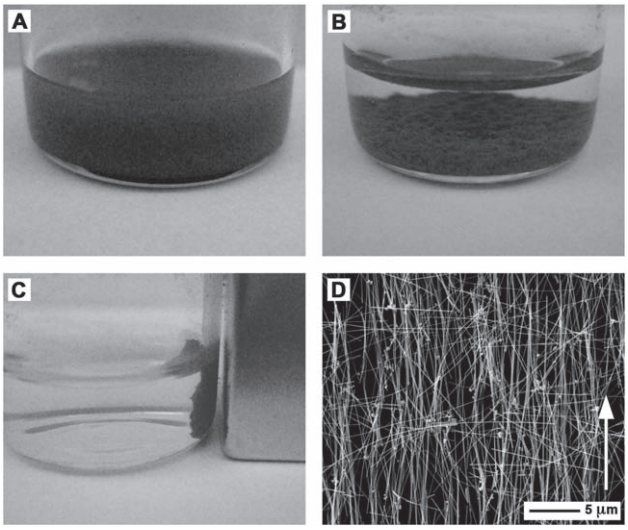

Figure 5. Digital images of A) Ag/Ni nanowires dispersed in ethanol, B) aggregated nanowires after being stored overnight, and C) nanowires attracted towards a small rare-earth magnet. D) SEM image of Ag/Ni nanowires after alignment on a silicon substrate using a C-shaped magnet. The magnetic field was applied along the direction indicated by the arrow.

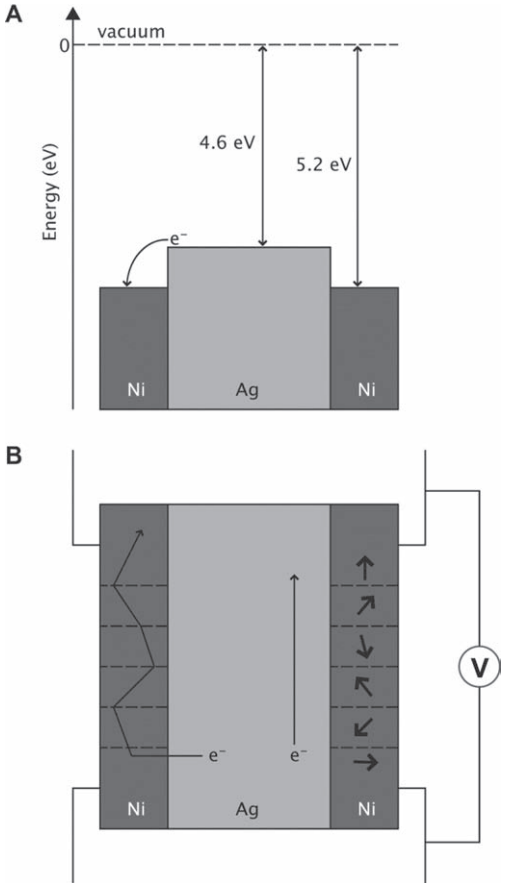

Figure 6. A) Diagram depicting the transfer of electrons from Ag to Ni due to the difference in work functions between these two metals. B) Diagram depicting the difference in conduction path for the electrons through the Ag core and Ni sheath. The randomized magnetic domains in Ni lead to increased scattering of electrons.

anisotropic morphology of the nanowires. If a handful of nanowires were aligned perpendicular to the field direction before the field was applied, then the net torque felt by the wire due to the magnetic field would be zero and no rotation would be induced. For those nanowires aligned diagonal to the field, perhaps they were in the process of rotating to align with the external magnetic field when the solvent was evaporated. In order to quantify the efficiency of this type of alignment method, a statistical distribution of the angle of the nanowires shown in Figure 5D relative to the magnetic field direction was obtained. The histogram summarizing this data is shown in Figure S2. Out of the 200 nanowires that were measured, a large majority of them were aligned within 10 degrees of the field direction. The distribution then dips as it nears 50 degrees and rises slightly at 90 degrees. This slight increase in the number of nanowires perpendicular to the field supports our theory discussed above.

2.4. Electrical Properties

The electrical conductivity of the Ag/Ni nanowires was determined by measuring the resistance of the nanowires using a two-probe method. Figure 4B shows the current–voltage (I–V) curve for the nanowires depicted in the inset SEM image in the same figure. Using SEM and atomic force microscopy (AFM) we determined that there were two nanowires spanning this electrode gap, which is expected given their ferromagnetic behavior (Figure S3). One of the nanowires had a diameter of 115 nm and the other a diameter of 80 nm. The resistance of these nanowires was determined from the slope of the I–V curve (1594 Ω) and the resistivity was calculated using the following equation,

$$\rho = \frac{R(A_1 + A_2)}{L} \tag{3}$$

where ρ is the resistivity, R is the resistance, L is the length between electrodes, A_1 is the cross-sectional area of the 115 nm nanowire, and A_2 is the area of the 80 nm nanowire. From the resistivity (5×10^{-4} Ω cm) we determined that the nanowires had an electrical conductivity of 2×10^3 S cm^{-1}. This value is about two orders of magnitude lower than the conductivities of bulk Ag (6.2×10^5 S cm^{-1}) and Ni (1.4×10^5 S cm^{-1}). This reduced conductivity can be explained as a result of the metal/metal interface created in our nanowires. By placing Ag and Ni in direct contact with each other we have created an avenue for electron transfer. In this case, electrons will prefer to transfer from the Ag core to the Ni sheath because of the difference in work functions between the two metals. **Figure 6**A illustrates this mechanism. Since the work function of Ni (≈5.2 eV) is larger than that of Ag (≈4.6 eV), its Fermi level is lower in energy.[38] Therefore, electrons in the Ag core will transfer to the Ni sheath in order to lower their overall energy. If both metals were single crystalline, the decrease in conductivity due to this transfer would be minimal since the resistivity of Ni (7×10^{-6} Ω cm) is only slightly higher than that of Ag (1.6×10^{-6} Ω cm). In our case, however, the Ni sheath was both ferromagnetic and polycrystalline,

which created many segregated magnetic domains with randomized orientations. An electron, which has an intrinsic spin, moving through this material will experience spin-dependent scattering, which is expected to greatly increase the resistance of the material. This phenomenon is similar to that of giant magnetoresistance (GMR) and we can use this concept to explain the reduced conductivity for our Ag/Ni nanowires. Generally, GMR occurs in systems that consist of alternating thin layers of ferromagnetic and nonmagnetic materials, in which, at room temperature and with no externally magnetic field applied, the spins of the magnetic layers are aligned antiparallel. An electron moving perpendicular to the layers will then experience spin-dependent scattering. In our case, once the electrons are transferred to the Ni sheath, their pathway through the material is impeded by the randomized magnetic domains, much like the electrons moving through the antiparallel layers. Figure 6B illustrates this mechanism. Therefore, the reduced conductivity of our nanowires can be explained through a combination of the difference in work functions and the spin-dependent scattering of electrons as they move through the Ni sheath.

2.5. Long-Term Storage

It is well known that elemental Ni is more susceptible to oxidation and corrosion than noble metals. In order for these Ag/Ni nanowires to be useful in applications such as nanoelectronics, their structure will need to be stable over a long period of time. As such, we were interested in how the long-term storage of these nanowires affected their structure. **Figure 7** shows TEM images of Ag/Ni nanowires stored by three different methods. The nanowires in Figure 7A were stored as a suspension in ultrapure water for six months. The inset shows a high-magnification TEM image of the nanowires illustrating their dramatic change in morphology. After six months of storage in water, a majority of the Ni on the nanowires had oxidized as indicated by the increase of lower contrast material on their surface.[35,39] This is likely due to the significant amount of dissolved oxygen in the water.[40] The nanowires in Figure 7B were stored as a suspension in absolute ethanol for six months and showed a slight decrease in their degree of oxidation. Finally, the nanowires in Figure 7C were stored as a dry sample on a TEM grid for six months. These nanowires were originally imaged immediately after synthesis, stored under ambient conditions, and re-imaged six months later. These nanowires show very little oxidation as indicated by the TEM image in the inset. Compared to the fresh nanowires in Figure 1C, these nanowires show a very similar surface morphology. We also collected EDX data for all three samples which is shown in Figure S4. There is a dramatic decrease in the height of the oxygen peak relative to the Ag and Ni peaks from the sample in Figure 7A to that in Figure 7C. This result is promising given that once the nanowires are deposited on a substrate, very little Ni oxidation will take place, which means these nanowires could be used in the fabrication and long-term use of nanoelectronics and other types of devices.

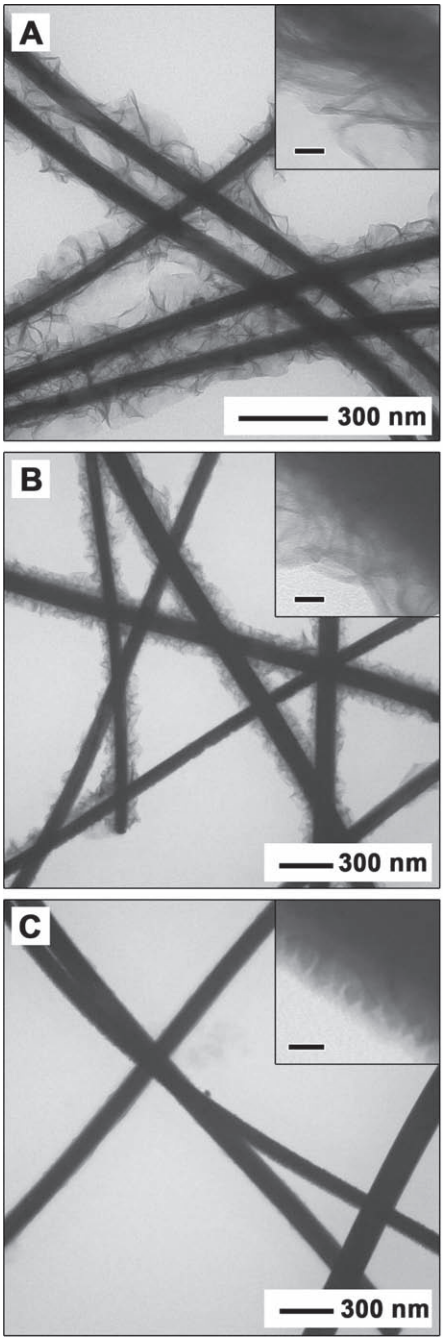

Figure 7. TEM images of Ag/Ni core/sheath nanowires stored under different conditions: A) as a suspension in ultrapure water; B) as a suspension in absolute ethanol; and C) as a dry sample on a TEM grid and placed in air. All the images were taken six months after sample preparation. The scale bars in the insets are 20 nm.

3. Conclusion

In summary, we have demonstrated the synthesis of Ag/Ni core/sheath nanowires using a two-step, solution-based method. The Ag/Ni nanowires had a rough surface morphology compared to the pristine Ag nanowires due to the growth of a polycrystalline Ni coating on the surface. We have confirmed the core/sheath structure of these nanowires through cross-sectional TEM imaging and EDX analysis. The

NANO MICRO small

nanowires exhibited magnetic hysteresis as demonstrated by their magnetization curves as well as macroscopic magnetic properties. We demonstrated the ability to control their alignment on a substrate by simply placing them in a magnetic field. We found that the Ag/Ni nanowires exhibit a reduction in electrical conductivity compared to Ag nanowires due to the creation of a metal/metal interface, which leads to the transfer of electrons from the highly electrically conductive Ag core to the polycrystalline ferromagnetic Ni sheath. These electrons then experience spin-dependent scattering, which tends to reduce the conductivity of the nanowires. Finally, we studied how their long-term storage affected their structure. We found that the nanowires stored on a substrate under ambient conditions had very little oxidation while those stored in a solvent (water or ethanol) showed signs of significant oxidation for the Ni coating. It is believed that these Ag/Ni core/sheath nanowires with their modified electrical conductivity and magnetic properties could eventually be used for the fabrication of electronic and display devices.

4. Experimental Section

Preparation of Ag Nanowires: To synthesize the Ag nanowires, we used a slightly modified $CuCl_2$-mediated method, which was described in detail in a previous study.[29] Briefly, 5 mL of ethylene glycol (EG, 99%, JT Baker) was preheated for 5 min in a 25 mL disposable vial in an oil bath set at 155 °C under magnetic stirring. To this, 65 μL of a 4 mM copper (II) chloride dihydrate, ($CuCl_2 \cdot 2H_2O$, 99+%, Aldrich) solution in EG was added. Then equal parts of a 0.094 M silver nitrate ($AgNO_3$, 99+%, Aldrich) solution in EG and a 0.282 M poly(vinyl pyrrolidone) (PVP, MW ≈ 55 000, Aldrich) solution in EG were mixed thoroughly and 3 mL of the mixture was quickly added to the vial. The vial was capped and the reaction was monitored by its color changes. The reaction was stopped once the sample became light tan with the wispy opalescence characteristic of Ag nanowires (about 45 min). The nanowires were washed once in EG/acetone (1:7 by volume) and centrifuged at 2000 rpm for 10 min. Then they were washed twice in water and centrifuged at 2000 rpm for 20 min to remove any byproducts such as Ag nanoparticles. The nanowires were stored in water until characterization and Ni coating. The concentration of Ag was determined by inductively coupled plasma mass spectrometry (ICP-MS).

Preparation of Ag/Ni Core/Sheath Nanowires: To coat the Ag nanowires with Ni sheaths, we first transferred them into EG. The nanowires were washed once in ethanol and centrifuged at 2000 rpm for 20 min. The concentrated nanowires in ethanol were then re-dispersed in 6 mL of EG for Ni coating. The dispersion was placed in a disposable vial and preheated in a 65 °C oil bath for 5 min with magnetic stirring. To this, a nickel acetate tetrahydrate ($(Ni(ac)_2 \cdot 4H_2O$, >99%, Fluka Analytical) and PVP solution was added to maintain a Ag:Ni ratio of 16:11. After 5 min, 0.5 mL of hydrazine monohydrate, ($N_2H_4 \cdot H_2O$, 98%, Aldrich), in EG (volume ratio $N_2H_4 \cdot H_2O$/EG = 80:720) was slowly added. The reaction proceeded for 15 min. The color of the nanowires changed to black and they formed large aggregates that adhered to the magnetic stir bar. The products were washed once in EG/acetone (1:7 by volume), centrifuged at 2000 rpm for 5 min and once in water, centrifuged at 2000 rpm for 20 min and re-dispersed in ethanol. The final products were cleaned twice in ethanol using magnetic separation and stored in ethanol until further characterization. SEM and TEM images of freshly prepared Ag/Ni core/sheath nanowires were taken immediately after synthesis to avoid any oxidation.

Structure Analysis: Samples for SEM were prepared by dropping a small amount of the suspension of nanowires on a silicon wafer. The samples were dried in the fume hood and washed with water in a gravity flow-cell before imaging. SEM images and EDX spectra were collected using a Nova NanoSEM 230 field-emission microscope (FEI, Hillsboro, OR) operated at an accelerating voltage of 15 kV. TEM samples were prepared by dropping a small amount of the suspension of nanowires on a carbon-coated copper grid. TEM images were obtained using a Hitachi H-7500 at an operating voltage of 100 kV. Cross-sectional TEM images were obtained by cross-sectioning a sample of Ag/Ni nanowires using a focused ion beam (FIB). The sample was then rough milled using 30 keV Ga^+ ion beam, followed by fine milling and polishing at 3.8 keV. The samples were thinned to ~50 nm thickness prior to imaging.

Measurement of Electrical Properties of Ag/Ni Core/Sheath Nanowires: Electrical conductivity of the Ag/Ni nanowires was measured using a two-probe method. The substrate was fabricated using photolithography. A plastic photomask was used to deposit 5-nm Ti and ≈70-nm Au on a Si/SiO_2 substrate. The substrate was then cleaned in boiling acetone for 3 min and sonicated in isopropanol for 30 s, followed by oxygen plasma treatment for 30 s. A diluted suspension of the nanowires in ethanol was drop casted onto the substrate and allowed to dry under ambient conditions. Electrical measurements were done using a Keithley 4200 SCS analyzer.

Measurement of Magnetic Properties of Ag/Ni Core/Sheath Nanowires: The hysteresis curve for the Ag/Ni sample was obtained using a Quantum Design Physical Property Measurement System. The Ag/Ni nanowires in ethanol were concentrated, loaded into a sample holder and allowed to dry before sealing with epoxy. The magnetic moment (emu) was then measured as a function of the applied magnetic field (Oe). Magnetic alignment was accomplished using a C-shaped magnet with a 2-cm opening and 0.05 T field. A small amount of Ag/Ni nanowires in butyl alcohol (99.96%, EMD Chemicals) was dropped onto a silicon wafer which had been placed directly between the two poles of the magnet. As the solvent evaporated, the nanowires had sufficient time to align (15–20 min). After washing in a gravity flow-cell, the nanowires were observed using a Nova NanoSEM 230 field-emission microscope (FEI, Hillsboro, OR) operated at an accelerating voltage of 15 kV.

Supporting Information

Supporting Information is available on the WWW under http://www.small-journal.com or from the author.

Acknowledgements

This work was supported by a grant from Applied Materials. Part of the research was conducted at the Nano Research Facility (NRF),

a member of the National Nanotechnology Infrastructure Network (NNIN), which is supported by the National Science Foundation under award ECS-0335765. Magnetic measurements were conducted at the Center for Materials Innovation (CMI) at Washington University in St. Louis. Transmission electron microscopy images were obtained at the Research Center for Auditory and Vestibular Studies, which is supported by the National Institutes of Health NIDCD Grant P30DC04665. Y.X. was also partially supported by the World Class University (WCU) program through the National Research Foundation of Korea funded by the Ministry of Education, Science and Technology (R32-20031).

[1] Y. Xia, P. Yang, Y. Sun, Y. Wu, B. Mayers, B Gates, Y. Yin, F. Kim, H. Yan, *Adv. Mater.* **2003**, *15*, 353.
[2] C. J. Murphy, T. K. Sau, A. M. Gole, C. J. Orendorff, J. Gao, L. Gou, S. E. Hunyadi, T. Li, *J. Phys. Chem. B* **2005**, *109*, 13857.
[3] J. Hu, T. W. Odom, C. M. Lieber, *Acc. Chem. Res.* **1999**, *32*, 435.
[4] Z. L. Wang, *Adv. Mater.* **2000**, *12*, 1295.
[5] J. Chen, B. J. Wiley, Y. Xia, *Langmuir* **2007**, *23*, 4120.
[6] Z. L. Wang, *Annu. Rev. Phys. Chem.* **2004**, *55*, 159.
[7] S. Bellucci, *Phys. Stat. Sol.* **2005**, *2*, 34.
[8] Y. S. Zhao, H. Fu, A. Peng, Y. Ma, Q Liao, J. Yao, *Acc. Chem. Res.* **2010**, *43*, 409.
[9] a) Y. Huang, X. Duan, Q. Wei, C. M. Lieber, *Science* **2001**, *291*, 630; b) N. I. Kovtyukhovaa, T. E. Mallouka, *Chem. Eur. J.* **2002**, *8*, 4354.
[10] a) S. A. Maier, P. G. Kik, H. A. Atwater, S. Meltzer, E. Harel, B. E. Koel, A. A. G. Requicha, *Nat. Mater.* **2003**, *2*, 229; b) M. Law, D. J. Sirbuly, J. C. Johnson, J. Goldberger, R. J. Saykally, P. Yang, *Science* **2004**, *305*, 1269; c) S. A. Maier, M. L. Brongersma, P. G. Kik, S. Meltzer, A. A. G. Requicha, H A Atwater, *Adv. Mater.* **2003**, *13*, 1501.
[11] E. Katz, I. Willner, *Angew. Chem. Int. Ed.* **2004**, *43*, 6042.
[12] A. K. Salem, P. C. Searson, K. W. Leong, *Nat. Mater.* **2003**, *2*, 668.
[13] K. Yu, J. Chen, *Nanoscale Res. Lett.* **2009**, *4*, 1.
[14] a) S. Sánchez, M. Pumera, *Chem. Asian J.* **2009**, *4*, 1402; b) S. Xu, Y. Qin, C. Xu, Y. Wei, R. Yang, Z. L. Wang, *Nat. Nanotech.* **2010**, DOI: 10.1038/nnano.2010.46.
[15] Y. Sun, Y. Yin, B. T. Mayers, T. Herricks, Y. Xia, *Chem. Mater.* **2002**, *14*, 4736; b) S. De, T. M. Higgins, P. E. Lyons, E. M. Doherty, P. N. Nirmalraj, W. J. Blau, J. J. Boland, J. N. Coleman, *ACS Nano* **2009**, *3*, 1767.
[16] J. Xu, A. Munari, E. Dalton, A. Mathewson, K. M. Razeeb, *J. Appl. Phys.* **2009**, *106*, 1.
[17] a) H. Staleva, S. E. Skrabalak, C. R. Carey, T. Kosel, Y. Xia, G. V. Hartlanda, *Phys. Chem. Chem. Phys.* **2009**, *11*, 5889; b) H. Ditlbacher, A. Hohenau, D. Wagner, U. Kreibig, M. Rogers, F. Hofer, F. R. Aussenegg, J. R. Krenn, *Phys. Rev. Lett.* **2005**, *95*, 1.
[18] G. Yu, X. Li, C. M. Lieber, A. Cao, *J. Mater. Chem.* **2008**, *18*, 728.
[19] a) Y. Huang, X. Duan, Q. Wei, C. M. Lieber, *Science* **2001**, *291*, 630; b) P. Yang, F. Kim, *ChemPhysChem* **2002**, *3*, 503.
[20] a) J. Lee, W. Hasan, M. H. Lee, T. W. Odom, *Adv. Mater.* **2007**, *19*, 4387; b) J. Yuan, H. Gao, F. Schacher, Y. Xu, R. Richter, W. Tremel, A. H. E. Muller, *ACS Nano* **2009**, *3*, 1441.
[21] H. Yu, M. Chen, P. M. Rice, S. X. Wang, R. L. White, S. Sun, *Nano Lett.* **2005**, *5*, 379.
[22] a) B. Lim, M. Jiang, P. H. C. Camargo, E. C. Cho, J. Tao, X. Lu, Y. Zhu, Y. Xia, *Science* **2009**, *324*, 1302; b) K. J. Major, C. De, S. O. Obare, *Plasmonics* **2009**, *4*, 61.
[23] X. Wang, A. Ren, K. Kahen, M. A. Hahn, M. Rajeswaran, J. Silcox, G. E. Cragg, A. L. Efros, T. D. Krauss, *Nature* **2009**, *459*, 686.
[24] E. C. Cho, P. H. C. Camargo, Y. Xia, *Adv. Mater.* **2010**, *22*, 744.
[25] J. Zhang, Y. Tang, K. Lee, M. Ouyang, *Science* **2010**, *327*, 1634.
[26] a) J. Zeng, J. Huang, C. Liu, C. Hao, Y. Lin, X. Wang, S. Zhang, J. Hou, Y. Xia, *Adv. Mater.* **2010**, *22*, 1936; b) G. Menagen, J. E. acdonald, Y. Shemesh, I. Popov, U Banin, *J. Am. Chem. Soc.* **2009**, *131*, 17406.
[27] S. Lin, S. Chen, Y. Chen, S. Cheng, *J. Alloys Compd.* **2008**, *449*, 232.
[28] a) Y. Sun, B. Gates, B. Mayers, Y. Xia, *Nano Lett.* **2002**, *2*, 165; b) Y. Sun, Y. Xia, *Adv. Mater.* **2002**, *14*, 833; c) Y. Sun, B. Mayers, T. Herricks, Y. Xia, *Nano Lett.* **2003**, *3*, 955; d) B. Wiley, Y. Sun, Y. Xia, *Langmuir* **2005**, *21*, 8077.
[29] K. E. Korte, S. E. Skrabalak, Y. Xia, *J. Mater. Chem.* **2008**, *18*, 437.
[30] Z. Peng, H. Yang, *Nano Today* **2009**, *4*, 143.
[31] Y. Du, M. Xu, J. Wu, Y. Shi, H. Lu, R. Xue, *J. Appl. Phys.* **1991**, *70*, 5903.
[32] E. P. Wohlfarth, *Ferromagnetic Materials*, (Ed: E. P. Wohlfarth) North-Holland, Amsterdam, The Netherlands, **1980**, p. 20.
[33] H. Wu, R. Zhang, X. Liu, D. Lin, W. Pan, *Chem. Mater.* **2007**, *19*, 3506.
[34] H. Wang, X. Jiao, D. Chen, *J. Phys. Chem. C* **2008**, *112*, 18793.
[35] A. C. Johnston-Peck, J. Wang, J. B. Tracy, *ACS Nano* **2009**, *3*, 1077.
[36] S. Chikazumi, *Physics of Magnetism*, Wiley, New York, **1964**, p. 19.
[37] J. Escrig, M. Daub, P. Landeros, K. Nielsch, D. Altbir, *Nanotechnology* **2007**, *18*, 1.
[38] D. E. Eastman, *Phys. Rev. B* **1970**, *2*, 1.
[39] P. Song, D. Wen, Z. X. Guo, T. Korakianitis, *Phys. Chem. Chem. Phys.* **2008**, *10*, 5057.
[40] R. Weiss, *Deep Sea Res.* **1970**, *17*, 721.

Received: May 12, 2010
Published online: July 30, 2010

